1

Activated biochar as an effective sorbent for organic and inorganic contaminants in water

4

5

Flavia Lega Braghiroli[1], Hassine Bouafif [2], Carmen Mihaela

Neculita[3], Ahmed Koubaa[1]

8

9

[1] Institut de recherche sur les forêts (IRF – Research Forest Institute), Université de Québec en

Abitibi-Témiscamingue (UQAT), 445 Boul. de l'Université, Rouyn-Noranda, Québec, QC J9X

5E4, Canada

[2] Centre Technologique des Résidus Industriels (CTRI, Technology Center for Industrial

Waste), Cégep de l'Abitibi-Témiscamingue (Abitibi-Témiscamingue College), 425 Boul. du

Collège Rouyn-Noranda, QC J9X 5E5, Canada

[3] Research Institute on Mines and the Environment (RIME), Université de Québec en Abitibi-

Témiscamingue (UQAT), 445 Boul. de l'Université, Rouyn-Noranda, QC J9X 5E4, Canada

18

19

20

21

* Corresponding author: (F.L. Braghiroli); Tel: +1 (819)-762-0931 ext. 1748; Fax: +1
(819)-762-0906; Email: Flavia.Braghiroli@uqat.ca

1

Abstract

Adsorption is acknowledged as effective for the removal of pollutants from drinking water and wastewater. Biochar, as a widely available material, holds promises for pollutant adsorption. So far, biochar has been found to be effective for multiple purposes, including carbon sequestration, nutrient storage, and water-holding capacity. However, its limited porosity restricts its use in water treatment. Activation of biochars, when performed at a high temperature (i.e., 900°C) and in presence of certain chemicals (H_3PO_4, KOH) and/or gases (CO_2, steam), improves the development of porosity through the selective gasification of carbon atoms. Physicochemical activation process is appropriate for the production of highly porous materials. As well, the morphological and chemical structure of feedstock together with pyro-gasification operating conditions for the biochar production can greatly impact the porosity of the final materials. The effectiveness of activated biochar as adsorbent depends on porosity and on some functional groups connected to its structure, both of these are developed during activation. This study provides a comprehensive synthesis of the effect of several activated biochars when applied to the treatment of organic and inorganic contaminants in water. Results show that high aromaticity and porosity are essential for the sorption of organic contaminants, while the presence of oxygen-containing functional groups and optimum pH are crucial for the sorption of inorganic contaminants, especially metals. Finally, although activated biochar is a promising option for the treatment of contaminants in water, further research is required to evaluate its performance with real effluents containing contaminants of emerging concern.

1. Introduction

Due to extensive anthropogenic activities, including industrial operations (such as mining), agricultural processes, and disposal of industrial wastewater materials, the concentration of contaminants in water is progressively increasing. A large number of anthropogenic and natural substances are present in water, including pharmaceuticals (prescriptions, over-the-counter drugs, and veterinary drugs), personal care products (fragrances, cosmetics, and sunscreens), steroid hormones, radioactive elements, metals (e.g., Pb, Hg, As), industrial chemicals (hydrocarbons and solvents), and pesticides. Most of these compounds have been recently defined as contaminants of emerging concern (CEC) because they are subject to critical action by regulatory agencies. CEC refer to naturally occurring, manufactured or manmade chemicals or materials that have been recently discovered, or persist in the environment for some time, posing toxicity concerns for living organisms (Sauvé and Desrosiers 2014). Potential leaching of organic and inorganic CEC from poorly managed residual waste sites (e.g., landfills, septic tanks) is also a concern. The main challenge is that, due to their very low concentrations, most wastewater treatment plants are not specifically designed to eliminate such contaminants, although they can have a chronic or long-term harmful impact on the environment. Given their persistence and continuous input, the CEC pass through treatment processes without being affected. Consequently, they end up in the aquatic environment and become dangerous to wildlife and probably are of concern with regard to drinking water (Sauvé and Desrosiers 2014; Petrie et al. 2015; Fairbairn et al. 2016).

Several regulatory bodies (e.g., United States Environmental Protection Agency, Health Canada, World Health Organization, etc.) monitor the levels of contaminants in wastewater treatment plants, drinking water, and effluent industries. Therefore, the discharge criteria should be below a level at which there is no known or expected risk to health. For example, according to
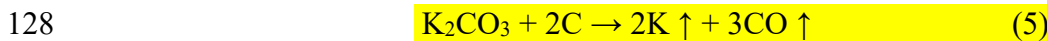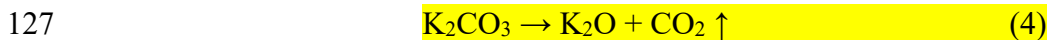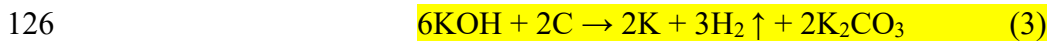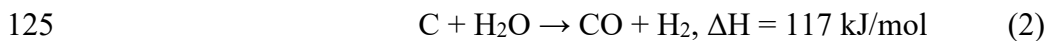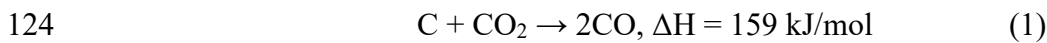
70 Health Canada, metals such as copper and iron can be present in drinking water at maximum

71 concentrations of 1.0 mg/L and 0.3 mg/L, respectively (Health Canada 2017). To maintain such low

72 levels of contaminants, several methods are employed, such as chemical precipitation (Li et al.

73 1999), ion exchange (Chiavola et al. 2012; Li et al. 2015), reverse osmosis (Greenlee et al. 2009;

74 Vaneeckhaute et al. 2012), electrochemical treatment (Martínez-Huitle and Ferro 2006; Moriwaki

75 et al. 2017), membrane processes (ultra-, micro- and nano-filtration) (Katsou et al. 2012; Sözen et

76 al. 2016), coagulation-floculation (Verma et al. 2012), flottation (Rubio et al. 2002), ozonation

77 (Wang et al. 2017), etc. Likewise, the combination of methods such as electro-Fenton process and

78 chemical precipitation (Ghosh et al. 2011), membrane bio-reactor with reverse osmosis (Dialynas

79 and Diamadopoulos 2009) or flotation with membrane filtration showed very high efficiency for

80 metals removal (Sudilovskiy et al. 2008). All these methods have advantages but they also have

81 disadvantages, including the chemicals and energy required, the increase in residual salinity of

82 treated water, the generation of toxic sludge, high cost, and incomplete contaminants removal

83 (Gaspard and Ncibi 2013).

84   One effective and widely used method for removing toxic contaminants from aqueous solutions

85 is adsorption process. It is the most versatile process to remove contaminants due to its simplicity

86 of design and ease of operation; it also provides high removal capacity (Babel and Kurniawan 2003;

87 Anastopoulos and Kyzas 2015; Hasan and Jhung 2015). The growing demand for adsorbent

88 materials for environmentally protective processes (mining and metallurgy) calls for more research

89 on the production of activated carbons from inexpensive materials (González-García 2018). The

90 thermochemical conversion of biomass feedstock (e.g., crop residues, manure, wood, wastewater

91 sludge) offers an efficient means to produce gaseous (biogas), liquid (bio-oil) and solid fuels (Fig.

92 1) compared to fossil-fuel-derived-materials. In various places, biomass waste thermochemical

93 conversion is an economically feasible alternative to deal with millions of tons of waste generated

94 by manufacturing activities in different industrial sectors (Dufour 2016; Pandey et al. 2015). The

95 solid fuels produced are also called biochar, defined by the International Biochar Initiative (IBI) as

96 a solid material obtained from the thermochemical conversion of biomass in a zero- or low-oxygen

97 environment (IBI 2012). Indeed, there is growing interest in research communities, biorefineries

98 and related industries in converting biochar into activated biochar due to: i) its low-cost availability;

99 ii) potential economic feasibility in large-scale production; iii) the increased profitability of existing

100 thermochemical conversion processes for the production of diversified products (biochar, bio-oil,

101 or syngas, and activated biochar); and iv) its effectiveness in several applications such as the

102 treatment (sorption) of drinking water and wastewater, energy storage, as electrodes in batteries

103 and supercapacitors, and as catalyst support (Fig. 1) (Tan et al. 2017).

104   Activation is considered the most common method for tailoring the pore structure of biochar.

105 Different pores sizes are created or developed by this approach: ultramicropores (< 0.7 nm),

106 micropores (between 0 and 2 nm), and mesopores (between 2 and 50 nm). An appropriate pore size

107 distribution is crucial in order to adsorb molecules of different sizes. There are three types of

108 activation: 1) physical (in presence of gases: CO_2 or vapor water), 2) chemical (biochars

109 impregnated with solutions of acids, salts, or bases) and 3) physicochemical (biochars impregnated

110 with solutions of acids, salts, or bases in presence of gases: CO_2 or vapor water) at high

111 temperatures (in an inert atmosphere), for the generation of a selective gasification of carbon atoms

112 and consequently, the development of porosity (Marsh and Rodríguez-Reinoso 2006). In physical

113 activation, the mechanism involved is as follows: the physical agents, CO_2 or steam, remove the

114 carbon atoms from the structure of the biochar according to Boudouard reaction Eq. 1 and Eq. 2,

115 respectively (Calo and Perkins 1987). On the contrary, in chemical activation, different reactions

occur simultaneously, depending on the chemical used. In general, chemicals such as acids (e.g., H_3PO_4) can act as a dehydration agent, whereas bases (e.g., KOH) can act as oxidant agents (Ozoemena and Chen 2016). Acids (e.g., H_3PO_4) can also act as catalysts, favoring activation, in the thermal treatment of biochar, whereas alkalis (e.g., KOH) can decompose in the form of metallic compounds (i.e., K, boiling-point elevation: 759°C) (Eqs. 3-6). In addition, the metallic compounds can be intercalated in the carbon lattice by thermal treatment, while gases (CO_2 and CO) could form and act as physical agents to the latter activation (Eqs. 4-6), thus favoring porosity development (Guo et al. 2002; Lozano-Castelló et al. 2007; Armandi et al. 2010).

$$C + CO_2 \rightarrow 2CO, \Delta H = 159 \text{ kJ/mol} \qquad (1)$$

$$C + H_2O \rightarrow CO + H_2, \Delta H = 117 \text{ kJ/mol} \qquad (2)$$

$$6KOH + 2C \rightarrow 2K + 3H_2 \uparrow + 2K_2CO_3 \qquad (3)$$

$$K_2CO_3 \rightarrow K_2O + CO_2 \uparrow \qquad (4)$$

$$K_2CO_3 + 2C \rightarrow 2K \uparrow + 3CO \uparrow \qquad (5)$$

$$K_2O + C \rightarrow 2K \uparrow + CO \uparrow \qquad (6)$$

The limited surface area and porosity of biochars restrain their potential to be applied in adsorptive processes. Removal of atrazine (the active substance in a pesticide) by KOH-activated biochar made from corn straw yielded a maximum sorption capacity 47 times higher compared to biochar due to its the higher surface area and higher aromaticity (Tan et al. 2016). Broiler litter biochar and activated broiler litter biochar were applied by Lima et al. (2010) as adsorbents for the removal of metals (Cu^{2+}, Cd^{2+}, Ni^{2+}) separately dispersed in water. In all cases, activated biochar performed better in the removal of metals, compared to biochars: 80% against 75% (Cu^{2+}), 85% against 22% (Cd^{2+}), and 96% against 10% (Ni^{2+}). Thus, porosity plays a major role in the performance of carbonaceous adsorbents. Indeed, activated biochars have higher surface area and

139 porosity compared to biochars as well as fewer functional groups connected to their carbonaceous

140 structure. Thus, the main mechanism involved in contaminant removal is related to physical

141 sorption (pores diffusion). However, depending on the chemical structures, characteristics of

142 activated biochar, and the type of contaminants, additional mechanisms for adsorbent-contaminant

143 interactions may also be involved during contaminant removal. In the case of inorganic

144 contaminants, several interactions (physical sorption, ion exchange, metals electrostatic attraction,

145 and metal precipitation) may be involved. Oppositely, in the case of organic pollutants, the main

146 mechanisms involved are partitioning or adsorption and electrostatic interactions (Ahmad et al.

147 2014; Liu et al. 2015; Tan et al. 2017).

148   In the following sections, the contaminants removed by activated biochars are discussed

149 separately (inorganics versus organics). A comprehensive list of such contaminants, together with

150 the type of wastewater used (e.g., synthetic vs. real effluent), the biochar feedstock, the activation

151 method used, as well as the corresponding surface area of the activated biochar, is compiled in

152 Table 1. This table also includes the adsorption capacity for contaminants by activated biochar

153 (mg/g), their experimental conditions, and a summary of the relevant results for each study.

154   **2.   Activated biochar for water treatment**

155   **2.1. Organic contaminants**

156   Among the organic contaminants listed in Table 1 are methylene blue, phenol, and dyestuff,

157 which have been extensively studied as contaminants removed through adsorption by the use of

158 activated carbons (Dąbrowski et al. 2005; Demirbas 2009; Rafatullah et al. 2010). Other organic

159 contaminants compiled in Table 1 are relatively new structures that have been recently studied,

160 since they are part of the emerging contaminants concern such as herbicides (Uchimiya et al. 2010)

161 and pharmaceutical compounds (Jung et al. 2013; Mondal et al. 2016b). In liquid-phase systems,

162   the adsorption capacity of activated carbons for aromatic compounds depends on a number of

163   factors: i) the nature of the adsorbent (e.g., its porous structure, ash content, and functional groups);

164   ii) the nature of adsorbate (e.g., its pK_a, polarity, functional groups, and molecular size); and finally,

165   iii) the solution conditions (e.g., pH, concentration, ion strength) (Haghseresht et al. 2002).

166   The greatest concern in water treatment is mixes of contaminants. Probable competition can

167   drastically reduce the adsorption capacity of adsorbents, even though contaminants are easily

168   removed from uni-component solutions. Jung et al. (2015a) studied the removal of single and

169   multiple contaminants present in solution such as diclofenac (DCF), naproxen (NPX), and

170   ibuprofen (IBP) through NaOH-activated biochar made from loblolly pine chips. The presence of

171   several contaminants in the same environment caused lower contaminant adsorption due to a

172   combination of a series of mechanisms: lower binding energy, polarity, and π-energy (i.e., energy

173   of molecular orbital of π electrons present in conjugated hydrocarbon systems), and electrostatic

174   repulsion from the contaminants occupying adsorption sites.

175   Furthermore, additional studies are needed for the treatment of real effluents that usually

176   contain several classes of contaminants. The majority of scientific works cited in Table 1 examined

177   single solutions prepared in the laboratory and studied mostly in batch sorption experiments.

178   Ranitidine hydrochloride (RH), however, was adsorbed from fixed-bed columns (Mondal et al.

179   2016a). In this testing, the adsorbate is in continuous contact with the adsorbent, a method that has

180   been widely used in industry for the removal of organic compounds by carbon adsorption

181   (Unuabonah et al. 2010; Karunarathne and Amarasinghe 2013). This contaminant is a medicine

182   normally used for gastric and intestinal problems, which is excreted through urine and feces and

183   therefore reaches a sewage system and ends up in rivers because wastewater plants cannot

184   completely remove it. Researchers also evaluated the influence of parameters such as bed depths,

185   initial concentration of contaminant, and volumetric flow rates on the performance of the adsorbent.

186   The main findings of sorption experiments with flow (column reactor type) were as follows: i) At

187   the highest bed-adsorbent height (3 cm), adsorption capacity was increased. A high amount of

188   adsorbent offered more binding sites, thus increasing the adsorption and other interactions with RH

189   molecules (Gupta et al. 1998; Al-Degs et al. 2009); ii) At the highest flow rate (6 mL/min),

190   adsorption capacity decreased due to adsorbate residence time insufficient to diffuse into the pores

191   or interact with the functional groups present in the adsorbent (Charumathi and Das 2012; Sadaf

192   and Bhatti 2014); iii) At the highest initial concentration, the sorption of the column was enhanced

193   due to the increased driving force for the mass transfer and RH loading rate (Han et al. 2007; Sancho

194   et al. 2012).

195   In addition, the type of activation (physical, chemical or physicochemical), diversity of

196   feedstock and pyro-gasification operating conditions applied for the preparation of biochars have

197   great effect on the porosity of activated biochars (Table 1). Steam-activated broiler litter biochar

198   synthesized after pyrolysis at 350°C and 700°C showed that for both materials the same surface

199   area of 335 m^2/g was attained. The chemical composition of broiler litter (high ash content) is

200   completely different from lignocellulosic precursors (low ash content). However, higher adsorption

201   capacity of deisopropylatrazine (a herbicide) was reached by applying high pyrolysis temperature

202   and subsequent activation (Uchimiya et al. 2010). Activated biochar has higher aromaticity, which

203   is an important parameter related to enhanced removal of organic pollutants due to its higher

204   hydrophobicity and π-π interactions (Boving and Zhang 2004; Moreno-Castilla 2004; Park et al.

205   2013). The same findings were observed for phenanthrene removal: faster initial sorption rate and

206   higher equilibrium concentration for phenanthrene adsorption were reported when using activated

207   biochar prepared at low pyrolysis temperature (300°C; $S_{BET} = 1250$ m^2/g), whereas stronger binding

208   with the sorbate was noted with the material pyrolyzed at 700°C ($S_{BET} = 57\ m^2/g$). The considerable

209   decrease in surface area of the activated biochar pyrolyzed at 700°C was due to the presence of

210   condensed aromatic structures, which were more stable and had fewer oxygen-containing groups

211   at the surface. Consequently, its carbon framework was resistant to thermal degradation (even when

212   impregnated with harsh chemicals, e.g., NaOH) inhibiting the development of a porous structure.

213   Although the activated biochar pyrolyzed at 700°C presented higher aromaticity, the material

214   having the highest surface area (pyrolyzed at 300°C) exhibited higher initial sorption efficiency

215   (156 mg/g) compared to a commercial activated carbon NORIT (130 mg/g) (Park et al. 2013).

216   In summary, surface area and aromaticity of activated biochars are the most important factors

217   for enhancing the sorption capacity of organic pollutants in water. Physicochemical and chemical

218   activation were found to be highly effective in producing these properties in activated biochars and,

219   consequently, increased their efficiency in the removal of organic compounds. Materials pore size

220   distribution [e.g., highly microporous ($\varnothing < 2.0$ nm) or even ultramicroporous ($\varnothing < 0.7$ nm)] play an

221   important role on the sorption of differently sized organic molecules. For example, iodine was

222   successfully adsorbed by activated biochars having smaller pores, compared to methylene blue,

223   which due to its high-size molecule, was found by most studies to need to be adsorbed by materials

224   with larger micropores and mesopores (Oh and Park 2002).

225   **2.1. Inorganic contaminants**

226   Most of the compounds included in the inorganic contaminant group are present in mining

227   effluents; they include both cations and anions Fe^{2+}, Fe^{3+}, Cu^{2+}, Ni^{2+}, Cd^{2+}, Zn^{2+}, As(III), and NH_4^+,

228   as well as Na^+ and PO_4^{3-}. In fact, globally, the mining industry is responsible for the generation of

229   the largest amount of waste material. The main problem is the exposure of chemically reactive

230   minerals to air and water, leading to contaminated mine drainage, either acid (AMD) or neutral

231   (CND) which generates pollution in surface water and groundwater (Westholm et al. 2014;

232   Rakotonimaro et al. 2017; Calugaru et al. 2018). In inorganic contaminants removal, in addition to

233   the porosity of the adsorbent materials, the presence of functional groups, such as carboxyl (–

234   COOH), phenol (–OH), and amino groups ($-NH_2$) on the surface of the adsorbents may help in the

235   removal of metals. In addition, the majority of studies listed in Table 1 reported that there is an

236   optimal pH at which activated biochars most effectively adsorbed inorganic contaminants in water

237   media.

238   The removal of Cu^{2+} was reported through the use of biochar and steam-activated biochar from

239   the *Miscanthus* plant (Shim et al. 2015). Surface sorption occurs beginning at pH 5, but the pH

240   level must be maintained below 7.5, since surface precipitation through $Cu(OH)_2$ formation takes

241   place at higher pH levels. The surface area of the activated biochar doubled compared to biochar

242   ($322\ m^2/g$ vs $181\ m^2/g$), while its polarity index [(O+N)/C] decreased. Cu^{2+} adsorption was better

243   fitted to the Freundlich and Langmuir models by using biochar and activated biochar, respectively,

244   but they presented almost the same adsorption capacity for Cu^{2+} in water (14 vs 15 mg/g). The

245   greater efficiency of biochar for Cu^{2+} could be because of the formation of metal complexes or

246   chelates due to the presence of more oxygenated functional groups connected to it compared to

247   activated biochar. Cu^{2+} may have been adsorbed through different mechanisms in both materials:

248   intra-particle diffusion and π-cation interactions in activated biochar, and surface complexation

249   with the metal in biochar.

250   The presence of several metals in the same environment may make the sorption of metal

251   contaminants quite complex once each metal is removed at different pH ranges. The adsorption of

252   three pollutants normally found in mining water, i.e., Fe^{2+}, Cu^{2+}, and As(V) within the pH range of

253   2–7, was reported by Banerjee et al. (2016). At lower pH (equal to 3), Fe^{2+} was highly adsorbed by

254   the activated biochar, whereas at higher pH, its adsorption decreased due to the formation of ferrous

255   species such as $[Fe(H_2O)_6]^{2+}$ and $[Fe(OH)(H_2O)_5]^+$, as well as the precipitation of $Fe(OH)_3$,

256   resulting in less adsorption of Fe^{2+} (Panday et al. 1985; Mohan and Pittman Jr. 2006; Hove et al.

257   2007; Banerjee et al. 2016). In relation to the contaminants As(V) and Cu^{2+}, the maximum removals

258   of 80% and 75%, respectively, were reached at pH 5 and 6, whereas low contaminants removal was

259   found at low pH. In other cases, it was reported that Cu^{2+} was the most adsorbed metal ion in single

260   solutions but the adsorption capacity of the activated biochar was reduced when other metals (Cd^{2+},

261   Ni^{2+}, Zn^{2+}) were found in the same environment (Lima et al. 2010). A probable metals competition

262   may have lowered the sorption of Cu^{2+}.

263   The type of pyro-gasification process and operating conditions were also found to have an

264   influence on the porosity of activated biochars and, consequently, on the removal of inorganic

265   contaminants. The proper choice of pyrolysis temperature (500 vs. 700°C) may influence the

266   porosity of biochars (50 vs. 300 m^2/g), and may have been responsible for the presence of

267   carboxylic and phenolic groups at the surface of the material, improving the cation-exchange and

268   complexation properties of the adsorbents for the removal of Fe^{3+} and Cu^{2+}, in addition to physical

269   sorption (Bouchelta et al. 2012). These findings were also confirmed by $MgCl_2.6H_2O$-activated

270   biochars prepared after first-step pyrolysis at 600°C, producing higher PO_4^{3-} (102 mg/g) removal

271   compared to a material made at 400°C (17 mg/g) (Takaya et al. 2016). Different biochars made

272   from slow and fast pyrolysis of the same feedstock also presented great differences in relation to

273   physicochemical properties and consequently, in metal ion uptake (Lima et al. 2010).

274   The type of activation was also found to play a role in the development of porosity of activated

275   biochars for the sorption of inorganic contaminants. For example, the removal of NH_4^+ from water

276   through activated biochar prepared at different types of activation using steam, CO_2, KOH, and

277 NH$_3$ was reported by Rambabu et al. (2015). By using NH$_4^+$ solution at 260 ppm, the sorption

278 capacity was found to be 55, 18, 149, and 57 mg/g, respectively. Chemical activation was shown

279 to be an effective approach for the development of porosity for the sorption of NH$_4^+$. However, the

280 presence of minerals (high ash content), the presence of oxygenated and nitrogenated functional

281 groups connected to the surface of activated biochar, and the chemical surface of modified materials

282 [e.g., Na$_2$S-modified biochar (Tan et al. 2016), ZnCl$_2$-activated biochar (Xia et al. 2016)] were also

283 found to be determinant for better heavy metals adsorption. In activated biochars, the overall metal

284 interaction mechanisms with these surface functionalities are electrostatic interactions, ion

285 exchange, surface complexation, and metal precipitation in addition to physical sorption.

286 **3. Conclusions and future research needs**

287 The present study reviewed the pertinent literature dedicated to the application of activated

288 biochars prepared from various feedstock and different pyro-gasification and activation operating

289 conditions, for the sorption of organic and inorganic contaminants in water media. The main

290 findings are outlined below:

291 i. The developed porosity (surface area and pore volume) and higher aromaticity were

292 important properties of activated biochars for the enhanced sorption of organic

293 contaminants in water due to higher hydrophobicity and π-π interactions. For inorganic

294 contaminants, activated biochar surface chemistry (e.g., the presence of oxygenated

295 functional groups, minerals) is an important property for enhancement of the interactions

296 with inorganics in water by various mechanisms: electrostatic interactions, ion exchange,

297 and surface complexation.

298 ii. The pH of the solution may also affect the sorption of organics and inorganics onto activated

299 biochar. Specifically, metals at precisely pH range can lead to precipitation mostly in a form

13

300 of hydroxides, which may solubilize afterwards depending on the pH conditions. Therefore,

301 an optimization study on the effect of the pH on the adsorption process is recommended.

302 iii. The pyro-gasification conditions, reactor design, as well as the quality of feedstock used for

303 the preparation of biochars have considerable influence on the textural properties (porosity)

304 of activated biochars as well on the environmental remediation applications. Optimization

305 of operating conditions and physicochemical characterization of biochars are recommended

306 for designing biochars for specific applications.

307 iv. The majority of studies on the application of activated biochars for the removal of organic

308 or inorganic contaminants in water were based on synthetic solutions in batch tests.

309 Therefore further studies should investigate column tests with real effluents characterized

310 by a mixture of contaminants of emerging concern (CEC), and various heavy metals from

311 mining industries, pharmaceuticals and pesticides, since they pose an increasing concern to

312 the environment, wildlife and drinking water systems.

313

322   **References**

323   Ahmad, M., Rajapaksha, A. U., Lim, J. E., Zhang, M., Bolan, N., Mohan, D., et al. (2014).

324   Biochar as a sorbent for contaminant management in soil and water: a review.

325   *Chemosphere*, *99*, 19–33. doi:10.1016/j.chemosphere.2013.10.071

326   Al-Degs, Y. S., Khraisheh, M. A. M., Allen, S. J., & Ahmad, M. N. (2009). Adsorption

327   characteristics of reactive dyes in columns of activated carbon. *Journal of Hazardous*

328   *Materials*, *165*(1–3), 944–949. doi:10.1016/j.jhazmat.2008.10.081

329   Anastopoulos, I., & Kyzas, G. Z. (2015). Composts as biosorbents for decontamination of various

330   pollutants: a review. *Water, Air, & Soil Pollution*, *226*(3). doi:10.1007/s11270-015-2345-2

331   Angın, D., Köse, T. E., & Selengil, U. (2013). Production and characterization of activated carbon

332   prepared from safflower seed cake biochar and its ability to absorb reactive dyestuff.

333   *Applied Surface Science*, *280*, 705–710. doi:10.1016/j.apsusc.2013.05.046

334   Armandi, M., Bonelli, B., Geobaldo, F., & Garrone, E. (2010). Nanoporous carbon materials

335   obtained by sucrose carbonization in the presence of KOH. *Microporous and Mesoporous*

336   *Materials*, *132*(3), 414–420. doi:10.1016/j.micromeso.2010.03.021

337   Babel, S., & Kurniawan, T. A. (2003). Low-cost adsorbents for heavy metals uptake from

338   contaminated water: a review. *Journal of Hazardous Materials*, *97*(1–3), 219–243.

339   doi:10.1016/S0304-3894(02)00263-7

340   Baçaoui, A., Yaacoubi, A., Dahbi, A., Bennouna, C., Ayele, J., & Mazet, M. (1998). Activated

341   carbon production from Moroccan olive wastes - influence of some factors.

342   *Environmental Technology*, *19*(12), 1203–1212. doi:10.1080/09593331908616780

343   Banerjee, S., Mukherjee, S., LaminKa-ot, A., Joshi, S. R., Mandal, T., & Halder, G. (2016).

344   Biosorptive uptake of Fe^{2+}, Cu^{2+} and As^{5+} by activated biochar derived from *Colocasia*

345   *esculenta*: isotherm, kinetics, thermodynamics, and cost estimation. *Journal of Advanced*

346   *Research*, *7*(5), 597–610. doi:10.1016/j.jare.2016.06.002

347 Bouchelta, C., Medjram, M. S., Zoubida, M., Chekkat, F. A., Ramdane, N., & Bellat, J.-P. (2012).

348   Effects of pyrolysis conditions on the porous structure development of date pits activated

349   carbon. *Journal of Analytical and Applied Pyrolysis*, *94*, 215–222.

350   doi:10.1016/j.jaap.2011.12.014

351 Boving, T. B., & Zhang, W. (2004). Removal of aqueous-phase polynuclear aromatic

352   hydrocarbons using aspen wood fibers. *Chemosphere*, *54*(7), 831–839.

353   doi:10.1016/j.chemosphere.2003.07.007

354 Calo, J. M., & Perkins, M. T. (1987). A heterogeneous surface model for the "steady-state"

355   kinetics of the boudouard reaction. *Carbon*, *25*(3), 395–407. doi:10.1016/0008-

356   6223(87)90011-X

357 Calugaru, I. L., Neculita, C. M., Genty, T., & Zagury, G. J. (2018). Metals and metalloids

358   treatment in contaminated neutral effluents using modified materials. *Journal of*

359   *Environmental Management*, *212*, 142–159. doi:10.1016/j.jenvman.2018.02.002

360 Charumathi, D., & Das, N. (2012). Packed bed column studies for the removal of synthetic dyes

361   from textile wastewater using immobilised dead *C. tropicalis*. *Desalination*, *285*, 22–30.

362   doi:10.1016/j.desal.2011.09.023

363 Chiavola, A., D'Amato, E., & Baciocchi, R. (2012). Ion exchange treatment of groundwater

364   contaminated by arsenic in the presence of sulphate. Breakthrough experiments and

365   modeling. *Water, Air, & Soil Pollution*, *223*(5), 2373–2386. doi:10.1007/s11270-011-

366   1031-2

367   Dąbrowski, A., Podkościelny, P., Hubicki, Z., & Barczak, M. (2005). Adsorption of phenolic

368   compounds by activated carbon - a critical review. *Chemosphere*, *58*(8), 1049–1070.

369   doi:10.1016/j.chemosphere.2004.09.067

370   Demirbas, A. (2009). Agricultural based activated carbons for the removal of dyes from aqueous

371   solutions: a review. *Journal of Hazardous Materials*, *167*(1–3), 1–9.

372   doi:10.1016/j.jhazmat.2008.12.114

373   Dialynas, E., & Diamadopoulos, E. (2009). Integration of a membrane bioreactor coupled with

374   reverse osmosis for advanced treatment of municipal wastewater. *Desalination*, *238*(1–3),

375   302–311. doi:10.1016/j.desal.2008.01.046

376   Ding, Z., Hu, X., Wan, Y., Wang, S., & Gao, B. (2016). Removal of lead, copper, cadmium, zinc,

377   and nickel from aqueous solutions by alkali-modified biochar: batch and column tests.

378   *Journal of Industrial and Engineering Chemistry*, *33*, 239–245.

379   doi:10.1016/j.jiec.2015.10.007

380   Dufour, A. (2016). *Thermochemical conversion of biomass for energy and chemical production*.

381   Hoboken, USA: John Wiley and Sons Inc.

382   El-Hendawy, A.-N. A., Samra, S. E., & Girgis, B. S. (2001). Adsorption characteristics of

383   activated carbons obtained from corncobs. *Colloids and Surfaces A: Physicochemical and*

384   *Engineering Aspects*, *180*(3), 209–221. doi:10.1016/S0927-7757(00)00682-8

385   Fairbairn, D. J., Arnold, W. A., Barber, B. L., Kaufenberg, E. F., Koskinen, W. C., Novak, P. J.,

386   et al. (2016). Contaminants of emerging concern: mass balance and comparison of

387   wastewater effluent and upstream sources in a mixed-use watershed. *Environmental*

388   *Science & Technology*, *50*(1), 36–45. doi:10.1021/acs.est.5b03109

389   Gaspard, S., & Ncibi, M. C. (2013). *Biomass for Sustainable Applications: Pollution Remediation*

390   *and Energy*. Cambridge, UK: Royal Society of Chemistry.

391   Ghosh, P., Samanta, A. N., & Ray, S. (2011). Reduction of COD and removal of Zn^{2+} from rayon

392   industry wastewater by combined electro-Fenton treatment and chemical precipitation.

393   *Desalination*, *266*(1–3), 213–217. doi:10.1016/j.desal.2010.08.029

394   Girgis, B. S., Soliman, A. M., & Fathy, N. A. (2011). Development of micro-mesoporous carbons

395   from several seed hulls under varying conditions of activation. *Microporous and*

396   *Mesoporous Materials*, *142*(2–3), 518–525. doi:10.1016/j.micromeso.2010.12.044

397   González-García, P. (2018). Activated carbon from lignocellulosics precursors: a review of the

398   synthesis methods, characterization techniques and applications. *Renewable and*

399   *Sustainable Energy Reviews*, *82*(1), 1393–1414. doi:10.1016/j.rser.2017.04.117

400   Greenlee, L. F., Lawler, D. F., Freeman, B. D., Marrot, B., & Moulin, P. (2009). Reverse osmosis

401   desalination: water sources, technology, and today's challenges. *Water Research*, *43*(9),

402   2317–2348. doi:10.1016/j.watres.2009.03.010

403   Guo, Y., Yang, S., Yu, K., Zhao, J., Wang, Z., & Xu, H. (2002). The preparation and mechanism

404   studies of rice husk based porous carbon. *Materials Chemistry and Physics*, *74*(3), 320–

405   323. doi:10.1016/S0254-0584(01)00473-4

406   Gupta, V. K., Srivastava, S. K., Mohan, D., & Sharma, S. (1998). Design parameters for fixed bed

407   reactors of activated carbon developed from fertilizer waste for the removal of some

408   heavy metal ions. *Waste Management*, *17*(8), 517–522. doi:10.1016/S0956-

409   053X(97)10062-9

410   Haghseresht, F., Nouri, S., Finnerty, J. J., & Lu, G. Q. (2002). Effects of surface chemistry on

411   aromatic compound adsorption from dilute aqueous solutions by activated carbon. *The*

412   *Journal of Physical Chemistry B*, *106*(42), 10935–10943. doi:10.1021/jp025522a

413 Hameed, B. H., & Rahman, A. A. (2008). Removal of phenol from aqueous solutions by

414   adsorption onto activated carbon prepared from biomass material. *Journal of Hazardous*

415   *Materials*, *160*(2–3), 576–581. doi:10.1016/j.jhazmat.2008.03.028

416 Hamid, S. B. A., Chowdhury, Z. Z., & Zain, S. M. (2014). Base catalytic approach: a promising

417   technique for the activation of biochar for equilibrium sorption studies of copper, Cu(II)

418   ions in single solute system. *Materials*, *7*(4), 2815–2832. doi:10.3390/ma7042815

419 Han, R., Wang, Y., Yu, W., Zou, W., Shi, J., & Liu, H. (2007). Biosorption of methylene blue

420   from aqueous solution by rice husk in a fixed-bed column. *Journal of Hazardous*

421   *Materials*, *141*(3), 713–718. doi:10.1016/j.jhazmat.2006.07.031

422 Hasan, Z., & Jhung, S. H. (2015). Removal of hazardous organics from water using metal-organic

423   frameworks (MOFs): Plausible mechanisms for selective adsorptions. *Journal of*

424   *Hazardous Materials*, *283*, 329–339. doi:10.1016/j.jhazmat.2014.09.046

425 Health Canada. (2017). *Guidelines for Canadian Drinking Water Quality. Summary Table* (pp. 9,

426   12). Ottawa, Canada. https://www.canada.ca/content/dam/hc-sc/migration/hc-sc/ewh-

427   semt/alt_formats/pdf/pubs/water-eau/sum_guide-res_recom/sum_guide-res_recom-

428   eng.pdf

429 Hove, M., van Hille, R. P., & Lewis, A. E. (2007). Iron solids formed from oxidation

430   precipitation of ferrous sulfate solutions. *AIChE Journal*, *53*(10), 2569–2577.

431   doi:10.1002/aic.11264

432 IBI. (2012). International Biochar Initiative. http://www.biochar-international.org/. Accessed 21

433   January 2018

434 Iriarte-Velasco, U., Sierra, I., Zudaire, L., & Ayastuy, J. L. (2016). Preparation of a porous

435   biochar from the acid activation of pork bones. *Food and Bioproducts Processing*, *98*,

436   341–353. doi:10.1016/j.fbp.2016.03.003

437   Jang, H. M., Yoo, S., Choi, Y.-K., Park, S., & Kan, E. (2018). Adsorption isotherm, kinetic

438   modeling and mechanism of tetracycline on *Pinus taeda*-derived activated biochar.

439   *Bioresource Technology*, *259*, 24–31. doi:10.1016/j.biortech.2018.03.013

440   Jung, C., Boateng, L. K., Flora, J. R. V., Oh, J., Braswell, M. C., Son, A., & Yoon, Y. (2015a).

441   Competitive adsorption of selected non-steroidal anti-inflammatory drugs on activated

442   biochars: experimental and molecular modeling study. *Chemical Engineering Journal*,

443   *264*, 1–9. doi:10.1016/j.cej.2014.11.076

444   Jung, C., Park, J., Lim, K. H., Park, S., Heo, J., Her, N., et al. (2013). Adsorption of selected

445   endocrine disrupting compounds and pharmaceuticals on activated biochars. *Journal of*

446   *Hazardous Materials*, *263*, *Part 2*, 702–710. doi:10.1016/j.jhazmat.2013.10.033

447   Jung, C., Phal, N., Oh, J., Chu, K. H., Jang, M., & Yoon, Y. (2015b). Removal of humic and

448   tannic acids by adsorption–coagulation combined systems with activated biochar. *Journal*

449   *of Hazardous Materials*, *300*, 808–814. doi:10.1016/j.jhazmat.2015.08.025

450   Jung, S.-H., & Kim, J.-S. (2014). Production of biochars by intermediate pyrolysis and activated

451   carbons from oak by three activation methods using CO_2. *Journal of Analytical and*

452   *Applied Pyrolysis*, *107*, 116–122. doi:10.1016/j.jaap.2014.02.011

453   Karunarathne, H. D. S. S., & Amarasinghe, B. M. W. P. K. (2013). Fixed bed adsorption column

454   studies for the removal of aqueous phenol from activated carbon prepared from sugarcane

455   bagasse. *10th Eco-Energy and Materials Science and Engineering Symposium*, *34*, 83–90.

456   doi:10.1016/j.egypro.2013.06.736

457   Katsou, E., Malamis, S., Kosanovic, T., Souma, K., & Haralambous, K. J. (2012). Application of

458   adsorption and ultrafiltration processes for the pre-treatment of several industrial

459   wastewater streams. *Water, Air, & Soil Pollution*, *223*(9), 5519–5534.

460   doi:10.1007/s11270-012-1255-9

461   Li, W., Zhang, L., Peng, J., Li, N., & Zhu, X. (2008). Preparation of high surface area activated

462   carbons from tobacco stems with K_2CO_3 activation using microwave radiation. *Industrial*

463   *Crops and Products*, *27*(3), 341–347. doi:10.1016/j.indcrop.2007.11.011

464   Li, W.-B., Song, Y.-B., Xu, H.-K., Chen, L.-Y., Dai, W.-H., & Dong, M. (2015). Ion-exchange

465   method in the collection of nitrate from freshwater ecosystems for nitrogen and oxygen

466   isotope analysis: a review. *Environmental Science and Pollution Research*, *22*(13), 9575–

467   9588. doi:10.1007/s11356-015-4522-7

468   Li, X. Z., Zhao, Q. L., & Hao, X. D. (1999). Ammonium removal from landfill leachate by

469   chemical precipitation. *Waste Management*, *19*(6), 409–415. doi:10.1016/S0956-

470   053X(99)00148-8

471   Lima, I. M., Boateng, A. A., & Klasson, K. T. (2010). Physicochemical and adsorptive properties

472   of fast-pyrolysis bio-chars and their steam activated counterparts. *Journal of Chemical*

473   *Technology & Biotechnology*, *85*, 1515–1521. doi:10.1002/jctb.2461

474   Lima, I. M., Boykin, D. L., Thomas Klasson, K., & Uchimiya, M. (2014). Influence of post-

475   treatment strategies on the properties of activated chars from broiler manure.

476   *Chemosphere*, *95*, 96–104. doi:10.1016/j.chemosphere.2013.08.027

477   Liu, W.-J., Jiang, H., & Yu, H.-Q. (2015). Development of biochar-based functional materials:

478   toward a sustainable platform carbon material. *Chemical Reviews*, *115*(22), 12251–12285.

479   doi:10.1021/acs.chemrev.5b00195

480   Lozano-Castelló, D., Calo, J. M., Cazorla-Amorós, D., & Linares-Solano, A. (2007). Carbon

481   activation with KOH as explored by temperature programmed techniques, and the effects

482   of hydrogen. *Carbon*, *45*(13), 2529–2536. doi:10.1016/j.carbon.2007.08.021

483   Malik, P. K. (2003). Use of activated carbons prepared from sawdust and rice-husk for adsorption

484   of acid dyes: a case study of acid yellow 36. *Dyes and Pigments*, *56*(3), 239–249.

485   doi:10.1016/S0143-7208(02)00159-6

486   Mandal, S., Sarkar, B., Igalavithana, A. D., Ok, Y. S., Yang, X., Lombi, E., & Bolan, N. (2017).

487   Mechanistic insights of 2,4-D sorption onto biochar: Influence of feedstock materials and

488   biochar properties. *Bioresource Technology*, *246*, 160–167.

489   doi:10.1016/j.biortech.2017.07.073

490   Marsh, H., & Rodríguez-Reinoso, F. (2006). *Activated carbon* (1st ed.). Amsterdam, NL:

491   Elsevier.

492   Martínez-Huitle, C. A., & Ferro, S. (2006). Electrochemical oxidation of organic pollutants for

493   the wastewater treatment: direct and indirect processes. *Chemical Society Reviews*, *35*(12),

494   1324–1340. doi:10.1039/B517632H

495   Mohan, D., & Pittman Jr., C. U. (2006). Activated carbons and low cost adsorbents for

496   remediation of tri- and hexavalent chromium from water. *Journal of Hazardous Materials*,

497   *137*(2), 762–811. doi:10.1016/j.jhazmat.2006.06.060

498   Mondal, S., Aikat, K., & Halder, G. (2016a). Ranitidine hydrochloride sorption onto superheated

499   steam activated biochar derived from mung bean husk in fixed bed column. *Journal of*

500   *Environmental Chemical Engineering*, *4*(1), 488–497. doi:10.1016/j.jece.2015.12.005

501   Mondal, S., Bobde, K., Aikat, K., & Halder, G. (2016b). Biosorptive uptake of ibuprofen by

502   steam activated biochar derived from mung bean husk: equilibrium, kinetics,

503   thermodynamics, modeling and eco-toxicological studies. *Journal of Environmental*

504   *Management*, *182*, 581–594. doi:10.1016/j.jenvman.2016.08.018

505   Moreno-Castilla, C. (2004). Adsorption of organic molecules from aqueous solutions on carbon

506   materials. *Carbon*, *42*(1), 83–94. doi:10.1016/j.carbon.2003.09.022

507   Moriwaki, H., Yamada, K., & Usami, H. (2017). Electrochemical extraction of gold from wastes

508   as nanoparticles stabilized by phospholipids. *Waste Management*, *60*, 591–595.

509   doi:10.1016/j.wasman.2016.07.010

510   Oh, G. H., & Park, C. R. (2002). Preparation and characteristics of rice-straw-based porous

511   carbons with high adsorption capacity. *Fuel*, *81*(3), 327–336. doi:10.1016/S0016-

512   2361(01)00171-5

513   Ozoemena, K. I., & Chen, S. (Eds.). (2016). *Nanomaterials in Advanced Batteries and*

514   *Supercapacitors*. Switzerland: Springer.

515   Panday, K. K., Prasad, G., & Singh, V. N. (1985). Copper(II) removal from aqueous solutions by

516   fly ash. *Water Research*, *19*(7), 869–873. doi:10.1016/0043-1354(85)90145-9

517   Pandey, A., Bhaskar, T., Stöcker, M., & Sukumaran, R. (Eds.). (2015). *Recent Advances in*

518   *Thermochemical Conversion of Biomass* (1st ed.). Amsterdam, NL: Elsevier.

519   Park, C. M., Han, J., Chu, K. H., Al-Hamadani, Y. A. J., Her, N., Heo, J., & Yoon, Y. (2017).

520   Influence of solution pH, ionic strength, and humic acid on cadmium adsorption onto

521   activated biochar: experiment and modeling. *Journal of Industrial and Engineering*

522   *Chemistry*, *48*, 186–193. doi:10.1016/j.jiec.2016.12.038

523   Park, J., Hung, I., Gan, Z., Rojas, O. J., Lim, K. H., & Park, S. (2013). Activated carbon from

524   biochar: influence of its physicochemical properties on the sorption characteristics of

525   phenanthrene. *Bioresource Technology*, *149*, 383–389. doi:10.1016/j.biortech.2013.09.085

526   Peng, H., Gao, P., Chu, G., Pan, B., Peng, J., & Xing, B. (2017). Enhanced adsorption of Cu(II)

527   and Cd(II) by phosphoric acid-modified biochars. *Environmental Pollution*, *229*, 846–853.

528   doi:10.1016/j.envpol.2017.07.004

529   Petrie, B., Barden, R., & Kasprzyk-Hordern, B. (2015). A review on emerging contaminants in

530   wastewaters and the environment: current knowledge, understudied areas and

531   recommendations for future monitoring. *Occurrence, fate, removal and assessment of*

532   *emerging contaminants in water in the water cycle (from wastewater to drinking water)*,

533   *72*, 3–27. doi:10.1016/j.watres.2014.08.053

534 Rafatullah, M., Sulaiman, O., Hashim, R., & Ahmad, A. (2010). Adsorption of methylene blue on

535   low-cost adsorbents: a review. *Journal of Hazardous Materials*, *177*(1–3), 70–80.

536   doi:10.1016/j.jhazmat.2009.12.047

537 Rajapaksha, A. U., Vithanage, M., Ahmad, M., Seo, D.-C., Cho, J.-S., Lee, S.-E., et al. (2015).

538   Enhanced sulfamethazine removal by steam-activated invasive plant-derived biochar.

539   *Journal of Hazardous Materials*, *290*, 43–50. doi:10.1016/j.jhazmat.2015.02.046

540 Rakotonimaro, T. V., Neculita, C. M., Bussière, B., Benzaazoua, M., & Zagury, G. J. (2017).

541   Recovery and reuse of sludge from active and passive treatment of mine drainage-

542   impacted waters: a review. *Environmental Science and Pollution Research*, *24*(1), 73–91.

543   doi:10.1007/s11356-016-7733-7

544 Rambabu, N., Rao, B. V. S. K., Surisetty, V. R., Das, U., & Dalai, A. K. (2015). Production,

545   characterization, and evaluation of activated carbons from de-oiled canola meal for

546   environmental applications. *Industrial Crops and Products*, *65*, 572–581.

547   doi:10.1016/j.indcrop.2014.09.046

548 Rengaraj, S., Moon, S.-H., Sivabalan, R., Arabindoo, B., & Murugesan, V. (2002). Agricultural

549   solid waste for the removal of organics: adsorption of phenol from water and wastewater

550   by palm seed coat activated carbon. *Waste Management*, *22*(5), 543–548.

551   doi:10.1016/S0956-053X(01)00016-2

552 Rostamian, R., Heidarpour, M., Mousavi, S. F., & Afyuni, M. (2015). Characterization and

553   sodium sorption capacity of biochar and activated carbon prepared from rice husk.

554   *Journal of Agricultural Science and Technology*, *17*(4), 1057–1069.

555　Rubio, J., Souza, M. L., & Smith, R. W. (2002). Overview of flotation as a wastewater treatment

556　　　technique. *Minerals Engineering*, *15*(3), 139–155. doi:10.1016/S0892-6875(01)00216-3

557　Sadaf, S., & Bhatti, H. N. (2014). Batch and fixed bed column studies for the removal of indosol

558　　　yellow BG dye by peanut husk. *Journal of the Taiwan Institute of Chemical Engineers*,

559　　　*45*(2), 541–553. doi:10.1016/j.jtice.2013.05.004

560　Saikia, R., Goswami, R., Bordoloi, N., Senapati, K. K., Pant, K. K., Kumar, M., & Kataki, R.

561　　　(2017). Removal of arsenic and fluoride from aqueous solution by biomass based

562　　　activated biochar: optimization through response surface methodology. *Journal of*

563　　　*Environmental Chemical Engineering*, *5*(6), 5528–5539. doi:10.1016/j.jece.2017.10.027

564　Sancho, J. L. S., Rodríguez, A. R., Torrellas, S. Á., & Rodríguez, J. G. (2012). Removal of an

565　　　emerging pharmaceutical compound by adsorption in fixed bed column. *Desalination and*

566　　　*Water Treatment*, *45*(1–3), 305–314. doi:10.1080/19443994.2012.692062

567　Sauvé, S., & Desrosiers, M. (2014). A review of what is an emerging contaminant. *Chemistry*

568　　　*Central Journal*, *8*(1), 15. doi:10.1186/1752-153X-8-15

569　Shim, T., Yoo, J., Ryu, C., Park, Y.-K., & Jung, J. (2015). Effect of steam activation of biochar

570　　　produced from a giant *Miscanthus* on copper sorption and toxicity. *Bioresource*

571　　　*Technology*, *197*, 85–90. doi:10.1016/j.biortech.2015.08.055

572　Sözen, S., Teksoy Başaran, S., Akarsubaşı, A., Ergal, I., Insel, G., Karaca, C., & Orhon, D.

573　　　(2016). Toward a novel membrane process for organic carbon removal—fate of slowly

574　　　biodegradable substrate in super fast membrane bioreactor. *Environmental Science and*

575　　　*Pollution Research*, *23*(16), 16230–16240. doi:10.1007/s11356-016-6795-x

576　Sudilovskiy, P. S., Kagramanov, G. G., & Kolesnikov, V. A. (2008). Use of RO and NF for

577　　　treatment of copper containing wastewaters in combination with flotation. *Desalination*,

578　　　*221*(1–3), 192–201. doi:10.1016/j.desal.2007.01.076

579   Sumalinog, D. A. G., Capareda, S. C., & de Luna, M. D. G. (2018). Evaluation of the

580   effectiveness and mechanisms of acetaminophen and methylene blue dye adsorption on

581   activated biochar derived from municipal solid wastes. *Journal of Environmental*

582   *Management*, *210*, 255–262. doi:10.1016/j.jenvman.2018.01.010

583   Takaya, C. A., Fletcher, L. A., Singh, S., Okwuosa, U. C., & Ross, A. B. (2016). Recovery of

584   phosphate with chemically modified biochars. *Journal of Environmental Chemical*

585   *Engineering*, *4*(1), 1156–1165. doi:10.1016/j.jece.2016.01.011

586   Tan, G., Sun, W., Xu, Y., Wang, H., & Xu, N. (2016). Sorption of mercury (II) and atrazine by

587   biochar, modified biochars and biochar based activated carbon in aqueous solution.

588   *Bioresource Technology*, *211*, 727–735. doi:10.1016/j.biortech.2016.03.147

589   Tan, X., Liu, S., Liu, Y., Gu, Y., Zeng, G., Hu, X., et al. (2017). Biochar as potential sustainable

590   precursors for activated carbon production: multiple applications in environmental

591   protection and energy storage. *Bioresource Technology*, *227*, 359–372.

592   doi:10.1016/j.biortech.2016.12.083

593   Uchimiya, M., Wartelle, L. H., Lima, I. M., & Klasson, K. T. (2010). Sorption of

594   deisopropylatrazine on broiler litter biochars. *Journal of Agricultural and Food*

595   *Chemistry*, *58*(23), 12350–12356. doi:10.1021/jf102152q

596   Unuabonah, E. I., Olu-Owolabi, B. I., Fasuyi, E. I., & Adebowale, K. O. (2010). Modeling of

597   fixed-bed column studies for the adsorption of cadmium onto novel polymer–clay

598   composite adsorbent. *Journal of Hazardous Materials*, *179*(1), 415–423.

599   doi:10.1016/j.jhazmat.2010.03.020

600   Vaneeckhaute, C., Meers, E., Michels, E., Christiaens, P., & Tack, F. M. G. (2012). Fate of

601   macronutrients in water treatment of digestate using vibrating reversed osmosis. *Water,*

602   *Air, & Soil Pollution*, *223*(4), 1593–1603. doi:10.1007/s11270-011-0967-6

603   Verma, A. K., Dash, R. R., & Bhunia, P. (2012). A review on chemical coagulation/flocculation

604   technologies for removal of colour from textile wastewaters. *Journal of Environmental*

605   *Management*, *93*(1), 154–168. doi:10.1016/j.jenvman.2011.09.012

606   Wang, F., Gao, B., Yue, Q., Bu, F., & Shen, X. (2017). Effects of ozonation, powdered activated

607   carbon adsorption, and coagulation on the removal of disinfection by-product precursors

608   in reservoir water. *Environmental Science and Pollution Research*, *24*(21), 17945–17954.

609   doi:10.1007/s11356-017-9451-1

610   Westholm, L. J., Repo, E., & Sillanpää, M. (2014). Filter materials for metal removal from mine

611   drainage—a review. *Environmental Science and Pollution Research*, *21*(15), 9109–9128.

612   doi:10.1007/s11356-014-2903-y

613   Wu, F.-C., & Tseng, R.-L. (2006). Preparation of highly porous carbon from fir wood by KOH

614   etching and CO_2 gasification for adsorption of dyes and phenols from water. *Journal of*

615   *Colloid and Interface Science*, *294*(1), 21–30. doi:10.1016/j.jcis.2005.06.084

616   Xia, D., Tan, F., Zhang, C., Jiang, X., Chen, Z., Li, H., et al. (2016). $ZnCl_2$-activated biochar from

617   biogas residue facilitates aqueous As(III) removal. *Applied Surface Science*, *377*, 361–

618   369. doi:10.1016/j.apsusc.2016.03.109

619

620

621

622

623 **Captions of the tables:**

624 **Table 1** Activated biochars applied to organic and inorganic (metals) contaminants removal from

625   water

626 **Captions of the figures:**

627 **Fig. 1** Thermochemical modification of biomass waste feedstock to produce biochar and activated

628   biochar, along with their most relevant applications

629

630

631

632

633

634

635

636

637

638

639

640

641

642

Table 1 Activated biochars applied to organic and inorganic (metals) contaminants removal from water

643

Contaminant	Biochar feedstock	Activated biochar / S_{BET} (m²/g)	Adsorption capacity activated biochar (mg/g)	Experimental conditions	Relevant results	Reference
Organic contaminants						
Methylene blue (MB) Iodine	Olive waste	Steam (-)	MB: 403 I: 1131	Synthetic effluent, T= 20°C	Adsorption of iodine and MB was enhanced by the use of highly porous activated biochars. Several parameters were involved in the development of porosity of activated olive waste biochar: lower pyrolysis temperature (e.g., 400°C), higher activation temperature (e.g., 900°C), and longer activation residence time (e.g., 2 h). The increase in activation temperature causes an opening and enlargement of the pores. However, iodine molecules were better adsorbed compared to MB due to its smaller size (well fitted in micropores)	(Baçaoui et al. 1998)
MB Phenol (Ph) Iodine (I) Pb^{2+}	Corncobs	Steam (607)	MB:- I: 325 Ph: 164 Pb^{2+}: 155	Synthetic effluent, pH ≤ 5.5 (Pb^{2+})	Steam-activated biochar developed microporosity when temperature is increased. Consequently, it exhibited good adsorption affinities in solutions having iodine, phenol, and MB. The removal of Pb^{2+} ions was highly dependent on pH solution. At pH ≥ 6.5, surface precipitation occurred. Higher adsorption of Pb^{2+} ions occurred at solution pH ≤ 5.5	(El-Hendawy et al. 2001)
MB Iodine	Rice straw	KOH (2410)	I: 1720 MB: 820	Synthetic effluent 0.02 N (I) and 1.2 g/L (MB)	Iodine adsorption increased with activation temperature between 600 and 800°C due to the development of micropores (< 1 nm), whereas MB adsorption increased between 800 and 900°C due to the development of larger micropores (up to 2 nm). These porous materials made at different conditions were favorable to the sorption of both contaminants: MB (molecule diameter of 1.5 nm) and iodine (molecule diameter of 0.5 nm, three times smaller than MB)	(Oh and Park 2002)
Phenol	Palm seed coat	CO_2 (577)	Batch: 18 Column: Synthetic effluent: 72; real effluent: 55	Batch and column testing, synthetic (10−60 mg/L) and real effluent (122 mg/L), equilibrium time 3 h, pH = 6.2, T = 27°C	The removal of phenol was greater at pH range 4−9. The adsorption of phenol on activated palm-seed-coat-biochar follows the Freundlich model based on the formation of a monolayer or film diffusion process. Adsorption of phenol in synthetic solution (72 mg/L) was higher in column tests compared to real phenol wastewater (55 mg/L). This may be due to the presence of other impurities or contaminants in wastewater that may have interfered in the phenol adsorption process	(Rengaraj et al. 2002)

Acid yellow 36	Sawdust (SD) and rice rusk (RH)	Steam SD: 516 RH: 272	SD: 184 RH: 87	Synthetic effluent 1000 mg/L, equilibrium time 1 h (SD) and 3h (RH), pH = 3, T = 30°C	Adsorption was highly dependent on contact time, adsorbent dose, and pH. The optimal pH for favorable adsorption of acid yellow 36 was 3 or below when high electrostatic attraction exists between the positively charged of the adsorbent and anionic dye. Two possible mechanisms for adsorption of dye into activated biochar are: 1) electrostatic interaction between the protonated group of carbon and acidic dye; and 2) chemical interaction between the adsorbate and the adsorbent	(Malik 2003)
Acid blue 74 Basic brown 1 MB p-nitrophenol 4-chlorophenol p-cresol phenol	Fir wood	KOH/CO_2 (2821)	359 1476 653 543 417 333 275	Synthetic effluent, T = 30°C	Physicochemical activation was a suitable technique for the production of highly porous materials. The presence of functional groups on the carbon surface (e.g., carbonyl, carboxylic, hydroxyl) indicates that there are many types of adsorbate–adsorbent interactions. Increasing CO_2 gasification time decreased micropore volume, but did not increase the adsorption capacity for phenol, for example. Contrary to other studies, these authors reported that the presence of higher amount of mesopores did not result in the material adsorbing a greater quantity of larger organic molecules. The low phenol adsorption might be due to the alteration of functional groups on the surface of the carbon through CO_2 gasification	(Wu and Tseng 2006)
Phenol	Rattan sawdust	KOH/CO_2 (-)	149	Synthetic effluent 25−200 mg/L, equilibrium time 4 h, pH < 8, T = 30°C	The maximum adsorption capacity of activated biochar was 149 mg/g. An important role on the sorption of phenol from aqueous solution was played by pH. Adsorption decreased at high pH values due to ionization of phenol molecules (pKa ≈ 9.89), whereas at acidic pH, the percentage of phenol removal was higher since its molecule did not dissociate and the dispersion interaction dominated	(Hameed and Rahman 2008)
MB Iodine (I)	Tobacco stems	K_2CO_3 (2557)	I: 1834 MB: 518	Synthetic effluent	Chemical activation was suitable for the production of activated biochar having a porous structure of 60% micropores and 40% meso- and macropores. The iodine number and MB adsorption increased to 1834 and 517 mg/g, respectively, with an increase of the K_2CO_3/biochar ratio from 0.5 to 1.5, and then the adsorption decreased to 1350 and 290 mg/g, respectively, at a ratio of 3. The decomposition of K_2CO_3 to K_2O and CO_2 molecules, which are then reduced by carbons to K and CO_2, causes the development of pores but only until a certain point; after that point, they widened and burned off	(Li et al. 2008)
Herbicide atrazine: deisopropylatrazine Cu^{2+}	Broiler litter	Steam (335)	-	Synthetic effluent 0−200 mg/L (atrazine) and 0−800 mg/L (Cu^{2+}), single and multiple contaminants, equilibrium time after 72 h, pH = 5.5	The pyrolysis temperature (700°C) and steam activation were responsible for increasing the aromaticity and surface area of activated broiler litter biochars. Deisopropylatrazine sorption was positively correlated with these parameters. In binary experiments, the presence of Cu^{2+} significantly diminished the	(Uchimiya et al. 2010)

					sorption of deisopropylatrazine, even though its sorption capacity was greater in single contaminant experiments	
MB	Oil seed hulls: soybean, cottonseed, sunflower, peanut; bean coats of lupine and broad beans	Steam (600)	18	Synthetic effluent 50−400 mg/L	The removal of MB was influenced by the acidic surface of activated biochar as well as its proportion of mesoporosity. Steam-activated biochar had high surface area with a high percentage of micropores that inhibited dye diffusion. In addition, its surface basicity (above $pH_{PZC} = 4$) resulted in low MB uptake (18 mg/g)	(Girgis et al. 2011)
Dyestuff	Safflower seed press cake	KOH (1277)	18	Synthetic effluent 20–100 mg/L, pH = 2, T = 25°C	Highly porous materials having surface area of $1277 m^2/g$ consisting of 75% of micropores had a strong effect on dyestuff removal. Maximum dyestuff removal was obtained at pH 2. At low pH, the negative charge on the surface of activated biochar was reduced due to the excess of protons in solution. Therefore, a positive charge surface of activated biochar favored the adsorption of dyestuff due to electrostatic attraction. The dyestuff removal efficiency was varied from 46 to 96% in presence of adsorbent amount from 0.05 to 0.6 g in 50 mL of dye solution	(Angın et al. 2013)
Bisphenol A (BPA) Atrazine (ATR) 17 α-ethinylestradiol (EE2) Pharmaceutical active compounds (PhACs) Sulfamethoxazole (SMX) Carbamazepine (CBM) Diclofenac (DCF) Ibuprofen (IBP)	Loblolly pine chips containing bark	NaOH (1360)	-	Synthetic effluent 10 μM, single and multiple contaminants, pH < pK_a, T = 20°C	The adsorption kinetics of these pharmaceutical compounds was very complex, especially when all species were found in the same environment and due to the desorption of some compounds having weak adsorption bonding energy. At pH values below their pKa, the adsorption of contaminants significantly increased; whereas at pH above pKa values, the adsorption was reduced significantly. The pseudo-second-order model implied that the mechanism involved in their removal was due to the chemical adsorption involving electronic forces through sharing or exchanging of electrons between the adsorbent and ionized species. The aromatic rings in all contaminants and adsorbents formed a π-system and enabled π-π interactions, which were positively correlated to the adsorption capacity for hydrophobic compounds	(Jung et al. 2013)
Phenanthrene (PAH)	Debarked loblolly pine chips	NaOH (1250)	156	Synthetic effluent 0.05−6.5 mg/L, equilibrium time 30 min, T = 25°C	Activated biochar prepared at low-temperature pyrolysis (300°C) presented a faster initial sorption rate and higher equilibrium concentration for phenanthrene removal. The sorption kinetics of the activated biochar seemed to be correlated with high surface area and pore volume. The presence of mesopores or larger pores were suitable for the sorption of larger contaminants. The activated biochar exhibited a good initial sorption (156 mg/g)	(Park et al. 2013)

Iodine	Oak	CO_2 (1126)	830	Synthetic effluent 0.1 N	Iodine adsorption indicated that the highest activation temperature had a great effect on the development of microporosity in activated biochars. The material synthesized at 900°C for 1 h had very high iodine number (830 mg/g) compared to commercial coal-based activated carbon (724 mg/g; S_{BET}: $1021 m^2/g$)	(Jung and Kim 2014)
Diclofenac (DCF) Naproxen (NPX) Ibuprofen (IBP)	Loblolly pine chips containing bark	NaOH (1360)	372 290 311	Synthetic effluent, single and multiple contaminants, pH = 7	The interaction energy between the surface of the activated biochar and the adsorbate was measured by ^{13}C nuclear magnetic resonance (NMR) analysis. DCF showed the highest adsorption capacity, interacting much better with the activated biochar compared to NPX and IBP. This strong interaction resulted in the occupation of effective adsorption sites as compared to the small-sized solutes (NPX and IBP) that blocked the pores. The coexistent tri-solute had a complex configuration. The presence of adsorption competitors lowered the adsorption capacity of the solutes due to low binding energy, low polarity, low π-energy, and electrostatic repulsion from cosolutes that occupied sites (in the case of deprotonated IBP that had very low adsorption capacity and negatively charged adsorbent surfaces)	(Jung et al. 2015a)
Humic acid (HA) Tannic acid (TA)	Loblolly pine chips containing bark	NaOH (1360)	9 19	Synthetic effluent 10 mg/L, single and multiple contaminants, pH = 7	Higher TA adsorption capacity onto activated biochar was observed due to its superior chemisorption tendencies and size-exclusion effects (its smaller molecular size provided access to inner pores present in the adsorbent). On the other hand, HA adsorption had much lower capacity due to hydrophobic interactions between the adsorbent and adsorbate	(Jung et al. 2015b)
Sulfamethazine (SMT)	Burcucumber plants	Steam (7)	38	Synthetic effluent 2.5−50 mg/L, pH = 3, T = 25°C	Steam-activated burcucumber biochar produced at 700°C showed the highest adsorption capacity (38mg/g) at pH 3. Chemiosorption was the major mechanism involved in SMT removal by activated biochar due to its very high ash content and very low surface area (7 m^2/g). The mechanisms involved were electrostatic interactions, but various other mechanisms may also have participated, including hydrophobicity, hydrogen bonding, and π-π interactions simultaneously	(Rajapaksha et al. 2015)

Methylene blue (MB)	Pork chop bones	H$_3$PO$_4$ (136) H$_2$SO$_4$ (140)	61 54	Synthetic effluent 50 mg/L, equilibrium time 1 h, pH = 5.8, T = 20°C	Higher impregnation rates enhanced microporosity when using H$_2$SO$_4$, whereas a dramatic reduction of porosity was reported when using H$_3$PO$_4$. The maximum uptake of MB was achieved at impregnation ratios of 0.2 mmol/g and 1 mmol/g using H$_3$PO$_4$ and H$_2$SO$_4$, respectively, which could be related to surface area in the 1.7-5.0nm pore range (large micropores and small mesopores)	(Iriarte-Velasco et al. 2016)
Ranitidine hydrochloride (RH)	Mung bean husk	Steam (405)	12	Column testing, synthetic effluent 100−200 mg/L, pH = 2, T = 28°C	The shape of the breakthrough curves on the adsorption of RH in column is strongly dependent on operation parameters. The highest adsorptive capacity of the sorbent was around 12 mg/g using bed height of 3 cm, flow rate of 2 mL/min, and RH concentration of 200 mg/L. It was reported that a variation in the initial concentration or flow rate changed the slope of the breakthrough curve of RH uptake	(Mondal et al. 2016a)
Ibuprofen (IBP)	Mung bean husk	Steam (405)	60	Synthetic effluent 1−100 mg/L, equilibrium time 2 h, pH = 2, T = 20°C	The optimized conditions for ∼ 99% IBP removal were as follows: adsorbent dose 0.1g/L, agitation speed 200 rpm, pH 2, initial IBP concentration 20 mg/L, equilibrium time 2 h, and temperature 20°C. Studies on thermodynamic parameters show that the removal of IBP was exothermic, spontaneous, and feasible. At lower temperature, adsorption was more likely to occur. The growth of *Scenedesmus abundans* was observed to be affected by IBP solution, whereas the activated biochar treated with IBP solution did not significantly affect its growth	(Mondal et al. 2016b)
Atrazine Hg^{2+}	Corn straw (*Zea mays L.*)	KOH (466)	92 5	Synthetic effluent 0.5–30 mg/L (atrazine) and 0–500 µg/L (Hg^{2+}), single and multiple contaminants, pH = 3 (atrazine) and pH = 4–6 (Hg^{2+}), T = 25°C	Na$_2$S-modified biochar showed the highest Hg^{2+} removal compared to KOH-activated biochar due to the formation of HgS precipitate. The presence of oxygen-containing functional groups on the char surface also had a positive effect on contaminant removal. For the atrazine removal, the KOH-activated biochar yield the maximum sorption capacity, 47 times higher than that of biochar. The main reasons could be the higher surface area, higher aromaticity, and porous structure with the presence of mesopores that favor the hydrophobicity effect and specific interactions. When both contaminants coexisted, the uptake removal for both materials was reduced, indicating the competition sorption between organic and inorganic adsorbates (probably both negatively charged). The surface functional groups (phenolic hydroxyl and carboxylic groups) played an important role in metals removal, with the formation of surface complexes between them. The main mechanisms involved in Hg^{2+} removal were electrostatic interactions, cation ion exchange, and Hg^{2+} precipitation. The polyaromatic surfaces of the sorbents influenced the π-π electron donor-receptor force,	(Tan et al. 2016)

					occurring mostly for materials that have more aromatic structures and higher surface areas	
Herbicide: 2,4-Dichlorophynoxy acetic acid (2,4-D)	Tea waste, burcucumber, oak wood, and bamboo	Steam (576)	59	Synthetic effluent 10−500 mg/L, pH = 7, T = 23°C	The highest pyrolysis temperature (700 vs. 400°C) seems to have an effect on increasing surface area of activated biochar, probably due to the opening of pore spaces with the removal of organic matter. The reason that steam-activated tea waste biochar adsorbed 2,4-D more efficiently compared to the biochar is the increased pore volume and pore diameter (micropores), higher surface area and aromatic carbon structure	(Mandal et al. 2017)
Tetracycline (TC)	Debarked loblolly pine	NaOH (960)	275	Synthetic effluent 10−100 mg/L, pH = 6, T = 20°C	NaOH-activated pine biochar showed higher TC adsorption capacity compared to biochar and various other activated biochars due to its developed porous structure having high surface area and mesopore volume (0.13 cm^3/g). Elovich kinetics and Freundlich isotherm models well fitted the data, indicating that hydrogen bonding and $\pi-\pi$ interaction on the heterogeneous surface might be the possible mechanisms while intra-particle diffusion would be the major limiting factor for TC adsorption on the activated biochar	(Jang et al. 2018)
Acetyl-para-aminophenol (acetaminophen or APAP) MB	Municipal solid waste	KOH (662)	APAP: 31 MB: 33	Synthetic effluent 50 mg/L, pH = 4 (APAP) and pH = 6.5 (MB), T = 30°C	The adsorption capacity of APAP highly decreased (about 89%) when pH increased from 2 to 12, whereas the variation of pH had little effect on MB adsorption. MB uptake was controlled by chemiosorption, whereas APAP adsorption was simultaneously controlled by physical (i.e., electrostatic interactions) and chemical interactions [i.e., chemical surface reactions with the oxygen-containing functional groups (−OH and –COOH)]	(Sumalinog et al. 2018)

Inorganic/Metal contaminants

Cu^{2+} Cd^{2+} Ni^{2+} Zn^{2+}	Broiler litter, alfalfa stems, switchgrass, corn cob, corn stover, guayule bagasse, guayule shrub, soybean straw	Steam (up to 793)	Removal of up to: 96% 85% 96% 40%	Synthetic effluent 1 mmol/L, single and multiple contaminants	Activated biochars showed improved uptake of metal ions compared to biochars. The improvement was associated with increased surface area (highly porous materials) and improved access of functional groups connected to the surface of activated biochars. Adsorption capacities were reduced once metal ions were in competition, compared to single metal solutions. Cu^{2+} was found to be the preferable metal ion to be adsorbed in single or multiple solutions. The pH was also found to play an important role in metals adsorption; precipitation of metals occurred at pH values higher than 6, in addition to adsorption	(Lima et al. 2010)
Cu^{2+} Fe^{3+}	Date pits	Steam (1467)	203 307	Synthetic effluent, equilibrium time 10 min, T = 18°C	Pyrolysis temperature (700°C) and activation hold time (4 h) were optimal parameter conditions applied for the production of	(Bouchelta et al. 2012)

					activated biochars reaching S_{BET} of 1467 m^2/g. High adsorption capacity of both metals was attributed to the presence of both carboxylic and phenolic groups on activated biochars, improving cation-exchange and complexation properties of such materials as well as greater surface area	
Cu^{2+}	Waste peels of mangosteen fruits	CO_2/KOH (367)	19	Synthetic effluent 50−100 mg/L, pH = 5.5, T = 30°C	Cu^{2+} cations in synthetic solution were adsorbed mainly by chemical interactions with the surface active sites of activated biochar. The adsorption uptake at equilibrium was found to increase with increasing initial Cu^{2+} concentration solutions. The higher the initial concentration, the larger was the driving force for mass transfer. The agitation time influenced the formation of an external film, which created a boundary layer over the surface of the adsorbent. Finally, the increase of the temperature (from 30 to 70°C) increased the velocity of adsorbate species toward the internal structure of the adsorbent	(Hamid et al. 2014)
Cu^{2+}	Broiler litter and broiler cake	Steam (up to 425)	104 49	Synthetic effluent 0.02 M, equilibrium time 24 h, pH = 4.8	Manure precursor presents high ash content which plays a role in the development of specific surface functionalities and consequently in the adsorption of Cu^{2+} ions. Adsorption is enhanced with the increase of the steam flow rate injected during activation (3 mL/min). Cu^{2+} uptake also increased with the presence of certain elements connected to the activated biochar: phosphorus, sulfur, calcium, and sodium	(Lima et al. 2014)
NH^{4+}	Canola meal	Steam (320) CO_2 (403) KOH (1230) NH_3 (19)	55 18 149 57	Synthetic effluent 260 mg/L, equilibrium time 30−240 min, pH = 9, T = 20°C	In terms of ammonium ion adsorption in relation to the type of activation at optimum pH = 9, KOH > NH_3 > steam > CO_2. Ammonium adsorption depended not only on pH and initial concentration but also on surface area and surface functional groups due to surface-related reactions such as adsorption, absorption, complexation, precipitation, and ion exchange	(Rambabu et al. 2015)
Na^+	Rice husk	KOH (K) (2201) Steam (S) (317) K/S (1169)	134 74 102	Synthetic effluent 0.2 M	Na^+ sorption increased with increasing surface area and pore volume. The K/S material was the most effective adsorbent for Na^+ sorption, having the highest percentage of micropores (effective pores to adsorb this cation). Researchers also reported intra-particle diffusion involved in the sorption process	(Rostamian et al. 2015)
Cu^{2+}	*Miscanthus* plant	Steam (322)	14	Synthetic effluent 0.2−150 mg/L, equilibrium time 120 h, pH = 6	Biochar made via slow pyrolysis presented a lower surface area compared to the activated biochar (181 vs. 322 m^2/g, respectively). However, Cu^{2+} sorption capacities were not significantly different. Fast sorption due to surface complexation dominated for biochar, whereas slow sorption due to intra-particle diffusion dominated for activated biochar. Both of them decreased the toxicity of Cu^{2+} but the activated material showed clear toxicity to *Daphnia magna*, possibly due to increased aromaticity upon steam activation	(Shim et al. 2015)

Fe^{2+} Cu^{2+} As(V)	*Colocasia esculenta* roots	Steam (102)	6.2 2.3 2.2	Synthetic effluent, Fe^{2+}: 50 mg/L, equilibrium time 30 min, pH 3, Cu^{2+}: 30 mg/L, equilibrium time 180 min, pH 5, As(V): 50 mg/L, equilibrium time 1440 min, pH 6 T = 25°C	Activated biochar was capable of removing 97% of Fe^{2+}, 95% of Cu^{2+}, and 84% of As(V) from aqueous solutions. The mechanism involved followed monolayer adsorption with maximum uptake of 6.2, 2.3, and 2.2 mg/g at initial concentrations of 50, 30, and 50 mg/L for Fe^{2+}, Cu^{2+}, and As(V), respectively. At pH 5 and 6, maximum removal of Cu^{2+} and As(V) was observed, whereas a decrease in Fe^{2+} adsorption was seen with an increase of pH from 3 to 7. Thus, activated biochar was capable of adsorbing various metals at different pHs	(Banerjee et al. 2016)
Pb^{2+} Cd^{2+} Cu^{2+} Zn^{2+} Ni^{2+}	Hickory chips	NaOH (873)	Batch: Multiple: 19 1.0 18 1.8 0.9 Single: Cu^{2+}: 54	Batch (2–250 mg/L) and column (100 mg/L) testing, single and multiple contaminants, equilibrium time 140 min, pH = 5, T = 20°C	NaOH-activated biochar had increased surface area, high oxygen-containing surface functional groups, and high cation-exchange capacity. Activated biochar also presented 2.6–5.8 times greater adsorption capacity for all heavy metal ions compared to biochar in single or multiple solutions. Pb^{2+} and Cu^{2+} were preferable metals from the competitive batch adsorption of mixed metal ions	(Ding et al. 2016)
PO$_4$$^{3-}$	Holm oak and greenhouse paprika waste	KOH (67.8) FeCl$_3$.6H$_2$O (-) MgCl$_2$.6H$_2$O (-)	26 102 25	Synthetic effluent 21–400 mg/L, pH = 7	The surface adsorption of biochars with or without pretreatment was sufficient for improving PO$_4$$^{3-}$ removal. An additional thermal treatment on Fe-impregnated biochars was not necessary, but low pH seems to influence Fe-loaded adsorbent for PO$_4$$^{-3}$ removal. Phosphate uptake capacities were enhanced from 2.1–3.6% to 66.4–70.3% by impregnation with magnesium. These findings show that the presence of minerals on activated biochar influences PO$_4$$^{3-}$ uptake much more than does porosity	(Takaya et al. 2016)
As(III)	Biogas residue from pig manure	ZnCl$_2$ (163)	28	Synthetic effluent 40 mg/L, equilibrium time 1.5 h, pH = 7, T = 25°C	ZnCl$_2$-activated biochar presented excellent adsorption efficiency for the removal of As(III) from solution. Adsorption was found to occur through ligand exchange (Zn^{2+}) which was loaded on hydroxyl groups present on the surface of the adsorbent (Zn-OH)) as well as through porous adsorption. Based on FTIR and XPS results, once in contact with As(III), the surface of the adsorbent becomes Zn-O-As(III). In this way, equilibrium was reached much faster and adsorption capacity increased significantly	(Xia et al. 2016)
Cd^{2+}	Debarked loblolly pine chips	NaOH (1151)	167	Synthetic effluent 2 mg/L, equilibrium time 6 h, pH = 7.5, T = 25°C	The maximum Cd^{2+} adsorption capacity was obtained at pH 7.5. The main mechanisms involved during Cd^{2+} adsorption were inner-sphere surface complexation and cation exchange. The ion strength was associated with particle aggregation and the affinity of the surface complexes with Cd^{2+}. The pseudo-second-order kinetic model fits the data well, whereas the sorption was controlled by a diffusion-limited mechanism	(Park et al. 2017)

Cd^{2+} Cu^{2+}	Pine sawdust	H_3PO_4 (900)	5 2	Synthetic effluent 1−10 mg/L, equilibrium time 6 h, pH = 4.5	The surface area of activated biochars increased with the increasing of pyrolysis temperature (from 200 to 650°C) during biochar production. Activated biochar had higher affinity for the sorption of heavy metals due to the increased surface area and oxygen-containing functional groups compared to biochars. Carboxyl and hydroxyl functional groups, and phosphorus-containing groups (P=O and P=OOH) formed complexes with metal ions, enhancing metals adsorption. Thus, sorption of metals by H_3PO_4-activated biochar was controlled by the mechanism of surface complexation	(Peng et al. 2017)
As(V) F^-	Perennial grass	KOH (1248)	Removal (%): 72 25	Synthetic effluent 100 mg/L (As(V)) and 25 mg/L (F^-), equilibrium time 60 min, pH = 7, T = 26°C	The optimal conditions for the maximum As(V) removal was: initial concentration, 100 mg/L; adsorbent dosage, 0.2 g/50 mL; and contact time of 60 min. In contrast, for F^- removal, the conditions were 25 mg/L, 0.2 g/50 mL and 60 min, respectively. Among these variables, adsorbent dosage was found to be the most influential parameter for the removal of both contaminants. Pseudo-first-order best fitted the data, indicating that adsorption was probably a chemiosorption process	(Saikia et al. 2017)

644